GEOPHYSICAL RESEARCH LETTERS, VOL. 39, L09803, doi:10.1029/2012GL051440, 2012

Reactive greenhouse gas scenarios: Systematic exploration of uncertainties and the role of atmospheric chemistry

Michael J. Prather,[1] Christopher D. Holmes,[1] and Juno Hsu[1]

Received 20 February 2012; revised 28 March 2012; accepted 5 April 2012; published 8 May 2012.

[1] Knowledge of the atmospheric chemistry of reactive greenhouse gases is needed to accurately quantify the relationship between human activities and climate, and to incorporate uncertainty in our projections of greenhouse gas abundances. We present a method for estimating the fraction of greenhouse gases attributable to human activities, both currently and for future scenarios. Key variables used to calculate the atmospheric chemistry and budgets of major non-CO_2 greenhouse gases are codified along with their uncertainties, and then used to project budgets and abundances under the new climate-change scenarios. This new approach uses our knowledge of changing abundances and lifetimes to estimate current total anthropogenic emissions, independently and possibly more accurately than inventory-based scenarios. We derive a present-day atmospheric lifetime for methane (CH_4) of 9.1 ± 0.9 y and anthropogenic emissions of 352 ± 45 Tg/y (64% of total emissions). For N_2O, corresponding values are 131 ± 10 y and 6.5 ± 1.3 TgN/y (41% of total); and for HFC-134a, the lifetime is 14.2 ± 1.5 y. **Citation:** Prather, M. J., C. D. Holmes, and J. Hsu (2012), Reactive greenhouse gas scenarios: Systematic exploration of uncertainties and the role of atmospheric chemistry, *Geophys. Res. Lett.*, *39*, L09803, doi:10.1029/2012GL051440.

[2] Increase in the atmospheric abundances of greenhouse gases (GHG) from pre-industrial era (PI) to present day (PD) is ascribed with high certainty as the major cause of recent climate change [*Santer et al.*, 1993; *Hegerl et al.*, 2007; *Barnett et al.*, 2008; *Zwiers and Hegerl*, 2008; *Min et al.*, 2011]. Attribution of the observed increases in three dominant long-lived GHG (CO_2, CH_4, N_2O) to human activities, however, has not been made with an equivalent level of certainty. Industrialization and land-use change have unquestionably driven most of these increases, but natural emissions and sinks, including atmospheric chemistry, can also have changed over the industrial era. Formal attribution including uncertainties of the observed GHG changes to humans requires a causal chain relating human activities to emissions to abundances to radiative forcing, one that includes propagation of uncertainties as outlined here.

[3] Projections of the long-lived, chemically controlled greenhouse gases – CH_4, N_2O, and the HFC-134a (CH_2FCF_3) – to year 2100 were made for the Intergovernmental Panel on Climate Change's (IPCC) Third Assessment Report (TAR) using anthropogenic emissions specified in the Special Report on Emissions Scenarios (SRES) [*Nakicenovic et al.*, 2000]. These included changes in atmospheric chemistry based on a multi-model study of global tropospheric chemistry done for the TAR [*Prather et al.*, 2001]. The IPCC 4th Assessment Report (AR4) [*Intergovernmental Panel on Climate Change* (*IPCC*), 2007] kept the SRES scenarios for these GHG and their projections from the TAR. With the IPCC 5th Assessment Report (AR5) being prepared for 2013, the community put together a new set of scenarios, the Representative Concentration Pathways (RCPs) [*Moss et al.*, 2010; *van Vuuren et al.*, 2011], which included a mapping of the emissions onto GHG abundances using a single parametric model [*Meinshausen et al.*, 2011b]. Projected abundances of CO_2 in climate assessments have in general included a measure of uncertainty such as the use of two carbon-cycle models to indicate a range in the TAR Appendix II [*Prentice et al.*, 2001; *Reisinger et al.*, 2010], but for reactive GHG a single best value is assumed. Climate model calculations for the 2013 IPCC AR5 (CMIP5) [*Lamarque et al.*, 2010; *Jones et al.*, 2011; *Meinshausen et al.*, 2011a, 2011b] (CMIP5, Coupled Model Intercomparison Project Phase 5, 2012, available at http://cmip-pcmdi.llnl.gov/cmip5/) are using mainly the scientific understanding of atmospheric chemistry and trace-gas budgets from the 2001 TAR to map anthropogenic emissions to abundances for long-lived GHG other than CO_2. Related studies for the AR5, the Atmospheric Chemistry and Climate MIP (ACCMIP), are investigating the relationship between emissions and composition for the reactive gases and aerosols with 3-D chemistry-climate models.

[4] Knowledge of uncertainty in current anthropogenic emissions is critical in projecting future abundances of N_2O and CH_4. For the industrially produced GHG, such as fossil-fuel CO_2 and synthetic HFCs, anthropogenic emissions estimates are generally accurate to 10% or better based on bottom-up inventory methods, although emissions of some synthetic fluorinated gases such as SF_6 remain greatly underestimated [*Levin et al.*, 2010]. Anthropogenic emission estimates from the agriculture, forestry and other land-use sectors (AFOLU), particularly for N_2O and CH_4, have uncertainties typically 25%–50% or larger [*Olivier and Berdowski*, 2001; *van Aardenne et al.*, 2001; *Denman et al.*, 2007; *Prather et al.*, 2009; *National Research Council*, 2010]. Thus, inventory-based estimates of these anthropogenic emissions, as in SRES and RCP, have uncertainties that would hinder quantitative attribution of the observed GHG increase to human activities. Both SRES and RCP define a set of scenarios with a range in anthropogenic emissions (e.g., RCP2.6, RCP4.5, RCP6.0, RCP8.5), each based on independent integrated assessment models. In the inventory-based method natural emissions are chosen to be constant and to

---

[1] Earth System Science Department, University of California, Irvine, California, USA.

Corresponding author: M. J. Prather, Earth System Science Department, University of California, 3329 Croul Hall, Irvine, CA 92697-3100, USA. (mprather@uci.edu)

0094-8276/12/2012GL051440

Table 1. Key Data for Pre-industrial and Present-Day Budgets of CH_4 and N_2O[a]

Quantity	CH_4 PI	CH_4 PD	N_2O PI	N_2O PD
abundance (ppb)	700 ± 25 (d2)	1795 ± 18 (e2)	270 ± 7 (d1)	323 ± 3.2 (e1)
growth (ppb/y)		5 ± 1 (f2)		0.8 ± 0.1 (f1)
lifetime (y)	9.5 ± 1.3 (P2)	9.1 ± 0.9 (H1)	142 ± 14 (P1)	131 ± 10 (t1)
emissions – total (Tg/y)	202 ± 28 (Q2)	554 ± 56 (K2)	9.1 ± 1.0 (Q1)	15.7 ± 1.1 (K1)
– natural (Tg/y)	202 ± 28 (Q2)	202 ± 35 (R2)	9.1 ± 1.0 (Q1)	9.1 ± 1.3 (R1)
– anthropogenic (Tg/y)		352 ± 45 (S2)		6.5 ± 1.3 (S1)

[a] Pre-industrial (PI) is year 1750. Present-day (PD) is year 2010. Abundances are tropospheric-mean mole fraction (ppb = 1 part in 10^9). PI CH_4 abundance does not include bias correction for different PI vs. PD standard scales [*Dlugokencky et al.*, 2005]. Emissions are Tg-CH_4 (10^{12} g) for CH_4, and Tg-N for N_2O. Uncertainties are denoted as ± one standard deviation (16%-to-84% = 68% confidence interval, see text). Quantities are selected from the larger list in Tables S1 and S2, with their location in those tables denoted in parentheses. Emissions sums may not balance due to the MC derived values.

exactly fill the gap between total emissions inferred from the model's adopted lifetime and the harmonized anthropogenic emissions, thus ensuring continuity with the observed abundances and trends at the start of the integration [*Prather et al.*, 2001; *Meinshausen et al.*, 2011a].

[5] Our approach to quantifying anthropogenic emissions is quite different from previous assessments and includes uncertainties throughout. Using a best estimate for current lifetime and atmospheric abundance, total PD sources are derived. Using observed pre-industrial abundances and model estimates of the PI-PD change in lifetimes, we calculate PI emissions. Current natural emissions are derived from these plus estimates of the change in natural emissions. For example, one study suggests natural CH_4 emissions may have decreased by 10% due to loss of wetlands [*Houweling et al.*, 2000], and we adopt a ±10% uncertainty in this change. We apportion the present-day budget into natural and anthropogenic sources with correlated uncertainties in each as shown in Table 1.

[6] First, we identify and quantify the key factors controlling past and future abundances of CH_4, N_2O, and HFC-134a. In terms of the Kyoto-specified GHG, other HFCs can be evaluated similarly to HFC-134a, while SF_6 and the perfluorocarbons are so long lived that their 21st century abundances are not impacted by uncertainties in atmospheric lifetimes. Primary factors include observations of past and present atmospheric abundances, recent growth rates, and data required to calculate global burdens and radiative forcing. Table S1 lists primary factors identified by lower-case letters (a)–(v) with numbers (e.g., (d1) = PI abundance of N_2O, (d2) = PI abundance of CH_4).[1] These are generally independent, and we assume that they have uncorrelated uncertainties, denoted in A1 both as ±absolute and ±relative (%) numbers and assumed to be the 16%-to-84% confidence interval and normally distributed (i.e., one-sigma about the mean). The values and uncertainties of the prime factors are derived from published studies, multiple models or lines of evidence, and expert judgment as noted in Table S1. Data derived primarily from atmospheric measurements, including air from polar ice sheets, are given asterisks (c*, d*, e*, f*, k*). Preindustrial (PI) is taken to be year 1750 per *IPCC* [2007], and present day is year 2010 with current trends based on years 2006–2010.

[7] Derived factors, such as atmospheric burdens, lifetimes and budgets, are listed in Table S2 and designated by upper-case letters (A)–(S). Their values and uncertainties are calculated from the primary values and their uncertainties. Where terms are additive, an absolute uncertainty is calculated from the square root of the sums of the squares of the absolute uncertainties; where multiplicative, a relative uncertainty is calculated similarly from the relative (%) uncertainties. This quadrature-sum method is included in Table S2 and assumes that all uncertainties are normal or long-normal. As a check we recalculated uncertainties with a Monte Carlo (MC) method: (1) a random number is used to select a single value for a primary factor from the probability distribution defined by the mean and standard deviation; (2) this process is repeated with different random numbers for all 40 primary factors in Table S1; (2) we calculate a single value for the each of the 46 derived factors in Table S2; (3) this process is repeated for 100,000 realizations; and (4) the mean and standard deviation in Table S2 are calculated from all realizations. The spreadsheet simple formulae and the MC agree except for emissions (Q–S), where uncertainties in the propagated quantities are highly correlated.

[8] Methylchloroform (MCF: CH_3CCl_3), a synthetic hydrochlorocarbon whose use has been phased out, has become the bellwether of tropospheric chemistry by providing an integrated measure of the reaction with tropospheric hydroxyl radical (OH) [*Prinn et al.*, 1992; *Spivakovsky et al.*, 2000]. The decay of tropospheric MCF since 2006 has followed a simple exponential decay that reflects the total atmospheric lifetime (k1) [*Montzka et al.*, 2011]. The atmospheric lifetime for a process is defined properly as the total atmospheric burden divided by total losses (e.g., against tropospheric OH, stratospheric photolysis), and thus inverse lifetimes (mean loss frequencies) are additive [*Forster et al.*, 2007; *Prather*, 2007]. By subtracting loss frequencies due to stratospheric photolysis (l1) and oceanic uptake (m1), a mean loss frequency (i.e., inverse lifetime) against tropospheric OH is derived (F1). This lifetime can be scaled to other species that react with OH by their relative reaction rates (h–i) [*Prather and Spivakovsky*, 1990; *Spivakovsky et al.*, 2000; *Lawrence et al.*, 2001]. Scaling the MCF decay rate to that of CH_4 and HFC-134a by reaction rates (i1–i2) assumes that total atmospheric burden scales with tropospheric mean abundance. The fill factor (c) defined here represents the reduced abundance of a gas in the stratosphere due to loss at high altitudes, it is calculated as the ratio of the integrated burden of the observed profile relative to that if it were uniformly mixed throughout the atmosphere. Thus, we correct the MCF decay with the fillz factor (c4) to correspond to the decay for a uniform MCF

---

[1] Auxiliary materials are available in the HTML. doi:10.1029/2012GL051440.

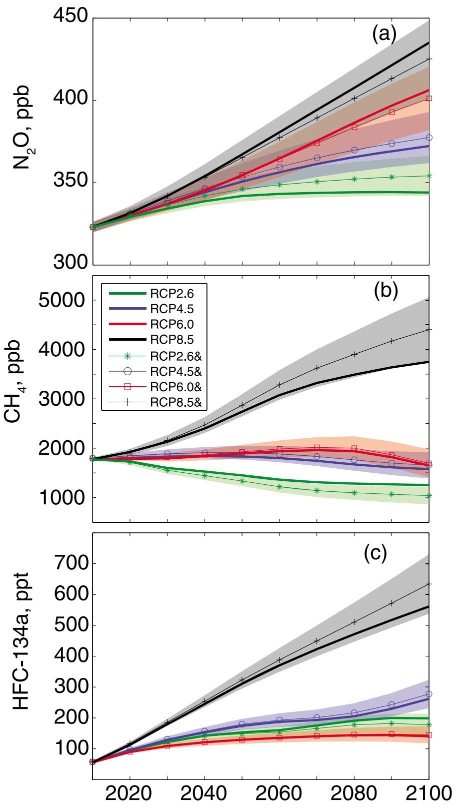

Figure 1. Projected atmospheric abundances for (a) N_2O, (b) CH_4 and (c) HFC-134a based on the four RCP emissions scenarios (2010–2100). The thick solid lines show the published RCP values: black, RCP8.5; red, RCP6.0; blue, RCP4.5; green, RCP 2.6 [*Meinshausen et al.*, 2011b]. Thin lines with markers show mean values derived here with shaded regions showing ±1 standard deviation based on the Monte Carlo calculations. Our results include all uncertainties listed in Table S1 and rescale the RCP emissions to match our derived year-2010 anthropogenic emissions.

abundance (F2), and then adjust the scaled OH lifetimes of CH_4 and HFC-134a (F3–F5) using their fill factors (c2–c3).

[9] The lifetime of CH_4 derived here, 9.1 ± 0.9 y, is about 5% longer with similar uncertainty as in AR4 [*Denman et al.*, 2007] (8.7 ± 1.3 y, quoted as 90%-confidence interval). Our uncertainty (~10%) is dominated by the ratio of the OH-reaction rates (i1). It would be much larger (>23%) if we took the separate uncertainties for each reaction from JPL-2010 [*Sander et al.*, 2010] as uncorrelated. Instead, we use an average of the recommended rates (i1) but take the uncertainty from the direct measurements of the ratio of these rates by DeMore and co-workers [*DeMore*, 1992; *Hsu and DeMore*, 1995], greatly reducing the uncertainty. Large uncertainties in some of the poorly understood, primary data can be readily shown to have little influence. For example, the lifetime of CH_4 against soil uptake (n1) used here (150 y ±33%) is based on TAR values, but use of a more recent evaluation (200 y ±50%, [*Curry*, 2007]) increases the CH_4 lifetime from 9.14 to 9.28 y, well within the one-sigma uncertainty range of ±10%.

[10] The total PD emissions for CH_4 and N_2O remain within 5% of those given in AR4 [*Denman et al.*, 2007]. For CH_4 the estimate of PD anthropogenic emissions here, 352 ± 45 Tg/y, is larger than that in the RCPs, ~335 Tg/y (the RCPs, harmonized in year 2005, have a spread of 24 Tg/y by 2010), but well within our uncertainty range. The major sources of uncertainty in our estimate are the PI-PD change in natural emissions and the OH-lifetime, both PI and PD. For N_2O the estimate of PD anthropogenic emissions here, 6.5 ± 1.3 Tg-N/y, is much smaller than that in the RCPs, ~7.9 Tg-N/y (the RCPs have a spread of 0.4 Tg-N/y by 2010), which fall just outside the one-sigma range. This difference is due to more recent evaluations of the PD N_2O lifetime [*Hsu and Prather*, 2010; *Fleming et al.*, 2011]. These top-down constraints on uncertainty in the current total anthropogenic emissions – 13% for CH_4 and 20% for N_2O – are a factor of two better than those derived from bottom-up inventory methods, even for developed countries – 25% for CH_4 and 50% for N_2O [*Prather et al.*, 2009] – but may be optimistic as there is limited research on the uncertainty in PI-PD changes of emissions and lifetime.

[11] With this model we project the future abundances of the greenhouse gases CH_4, N_2O, and HFC-134a initialized with observed values in year 2010 and integrated to 2100 using the RCP anthropogenic emissions (see Figure 1). For each of the 100,000 MC realizations, a value for PD (year 2010) anthropogenic emissions of CH_4 and N_2O is derived. For each of the four RCPs, all projected emissions of CH_4 and N_2O are scaled by a single factor to match the MC value at 2010, and we assume no future change in natural emissions. To project the change in lifetime to 2100 in this study we use only the self-feedback factors (q1, s1) and very simple estimates with uncertainties of the impacts of other factors on lifetime (r1, u1). A significant, but not assessed, uncertainty in projecting future CH_4 lies with the RCP projections of other anthropogenic reactive gases considered pollutants, such as nitric oxide, carbon monoxide, and aerosols. These species control tropospheric OH, and there remains considerable uncertainty in their future emissions for any scenario [*Cofala et al.*, 2007; *Kloster et al.*, 2010]. For each of the 100,000 MC realizations, a single time-line from 2010 to 2100 is generated for each gas and each RCP. Every decade the MC ensemble mean and spread (±standard deviation) are plotted in Figure 1, where our projected CH_4, N_2O and HFC-134a abundances and uncertainties are compared with the single-valued RCPs [*Meinshausen et al.*, 2011b].

[12] In spite of the 20% difference in anthropogenic N_2O emissions, our abundances track the RCP abundances in Figure 1a for each scenario over the first decades because both have constrained total emissions to match current abundance and growth rate with the chosen lifetime. The differences at 2100 reflect our model's larger self-feedback factor (s1) and longer lifetime (l1): reducing the larger abundances in RCP8.5 and RCP6.0, while increasing the smaller abundances in RCP2.6 and RCP 4.5. Thus, our analysis predicts a tight range of future N_2O abundances for the same range of anthropogenic emissions, but the uncertainty range includes the larger spread of the RCP abundances. Results for CH_4 in Figure 1b show the opposite: both the large increases projected for RCP8.5 and the large decreases projected for RCP2.6 are enhanced in our analysis. The cause is likely similar to that for N_2O, but with differences in lifetime and feedback amplifying the changes, particularly for RCP8.5 with the largest emissions increases. Another possible cause of CH_4 differences in Figure 1b is

that the RCP model includes a temperature dependence of the OH-CH_4 reaction, reducing the lifetime with global warming. This factor was not included here because it would presume that RCPs correctly project climate change and further studies are needed to relate the global mean to the pattern of temperature change over the primary regions where CH_4 is destroyed. As noted above, the synthetic greenhouse gas HFC-134a has no natural emissions and hence the RCP emissions cannot be scaled using this method. The range in projected HFC-134a abundances shown for each RCP in Figure 1c is caused primarily by uncertainty in the tropospheric OH lifetime and its response to changing CH_4 abundance.

[13] Quantitative attribution of a change in N_2O or CH_4 abundances to human activities, from pre-industrial to present day or for future changes, could be made with a statistical model such as this; however, a more careful assessment of uncertainty in the change of natural emissions and lifetime is needed. In addition, uncertainties in inventory-based emissions from the AFOLU sector would need to be included explicitly (e.g., Bayesian methods). Such an approach could make a quantitative attribution to the primary anthropogenic emissions of N_2O and CH_4. The importance of other anthropogenic emissions on the lifetimes (p1, u1) or of global change as a whole (e.g., climate, pollution, land use) should also be included, but will need a wider approach.

[14] The values derived here represent our current best estimates, and we expect them to change with new scientific results and a broader community evaluation of the uncertainties. Even the scope of primary quantities can expand. Thus, we provide in the auxiliary material both the spreadsheet for calculation of many derived quantities and the Matlab code used in the Monte Carlo calculation of emissions. A clear advantage of the approach outlined here is that new science is readily incorporated and that critical variables driving the uncertainty can be identified and become a research focus.

[15] **Acknowledgments.** This research was supported by NASA NNX08AR25G, NASA NNX09AJ47G, DOE DE-SC0007021, and the Kavli Chair in Earth System Science. We thank Ed Dlugokencky, two anonymous reviewers, and other colleagues involved with the RCPs and in the preparation of the IPCC AR5 for discussions that helped initiate and focus this work, and for a careful reading. All data reported here are archived in the auxiliary material.

[16] The Editor wishes to thank two anonymous reviewers for assisting with the evaluation of this paper.

References

Barnett, T. P., et al. (2008), Human-induced changes in the hydrology of the western United States, *Science*, *319*(5866), 1080–1083, doi:10.1126/science.1152538.

Cofala, J., M. Amann, Z. Klimont, K. Kupiainen, and L. Hoglund-Isaksson (2007), Scenarios of global anthropogenic emissions of air pollutants and methane until 2030, *Atmos. Environ.*, *41*, 8486–8499, doi:10.1016/j.atmosenv.2007.07.010.

Curry, C. L. (2007), Modeling the soil consumption of atmospheric methane at the global scale, *Global Biogeochem. Cycles*, *21*, GB4012, doi:10.1029/2006GB002818.

DeMore, W. B. (1992), Relative rate constants for the reactions of OH with methane and methyl chloroform, *Geophys. Res. Lett.*, *19*(13), 1367–1370, doi:10.1029/92GL01278.

Denman, K. L., et al. (2007), Couplings between changes in the climate system and biogeochemistry, in *Climate Change 2007: The Physical Science Basis. Contribution of Working Group I to the Fourth Assessment Report of the Intergovernmental Panel on Climate Change*, edited by S. Solomon et al., pp. 499–587, Cambridge Univ. Press, Cambridge, U. K.

Dlugokencky, E. J., R. C. Myers, P. M. Lang, K. A. Masarie, A. M. Crotwell, K. W. Thoning, B. D. Hall, J. W. Elkins, and L. P. Steele (2005), Conversion of NOAA atmospheric dry air CH_4 mole fractions to a gravimetrically prepared standard scale, *J. Geophys. Res.*, *110*, D18306, doi:10.1029/2005JD006035.

Fleming, E. L., C. H. Jackman, R. S. Stolarski, and A. R. Douglass (2011), A model study of the impact of source gas changes on the stratosphere for 1850–2100, *Atmos. Chem. Phys.*, *11*(16), 8515–8541, doi:10.5194/acp-11-8515-2011.

Forster, P., et al. (2007), Changes in atmospheric constituents and in radiative forcing, in *Climate Change 2007: The Physical Science Basis. Contribution of Working Group I to the Fourth Assessment Report of the Intergovernmental Panel on Climate Change*, edited by S. Solomon et al., pp. 129–234, Cambridge Univ. Press, Cambridge, U. K.

Hegerl, G. C., F. W. Zwiers, P. Braconnot, N. P. Gillett, Y. Luo, J. A. Marengo-Orsini, N. Nicholls, J. E. Penner, and P. A. Stott (2007), Understanding and attributing climate change, in *Climate Change 2007: The Physical Science Basis. Contribution of Working Group I to the Fourth Assessment Report of the Intergovernmental Panel on Climate Change*, edited by S. Solomon et al., pp. 663–745, Cambridge Univ. Press, Cambridge, U. K.

Houweling, S., F. Dentener, and J. Lelieveld (2000), Simulation of preindustrial atmospheric methane to constrain the global source strength of natural wetlands, *J. Geophys. Res.*, *105*(D13), 17,243–17,255, doi:10.1029/2000JD900193.

Hsu, K. J., and W. B. DeMore (1995), Rate constants and temperature dependences for the reactions of hydroxyl radical with several halogenated methanes, ethanes, and propanes by relative rate measurements, *J. Phys. Chem.*, *99*(4), 1235–1244, doi:10.1021/j100004a025.

Hsu, J., and M. J. Prather (2010), Global long-lived chemical modes excited in a 3-D chemistry transport model: Stratospheric N_2O, NOy, O_3 and CH_4 chemistry, *Geophys. Res. Lett.*, *37*, L07805, doi:10.1029/2009GL042243.

Intergovernmental Panel on Climate Change (IPCC) (2007), *Climate Change 2007: The Physical Science Basis. Contribution of Working Group I to the Fourth Assessment Report of the Intergovernmental Panel on Climate Change*, edited by S. Solomon et al., 996 pp., Cambridge Univ. Press, Cambridge, U. K.

Jones, C. D., et al. (2011), The HadGEM2-ES implementation of CMIP5 centennial simulations, *Geosci. Model Dev.*, *4*(3), 543–570, doi:10.5194/gmd-4-543-2011.

Kloster, S., F. Dentener, J. Feichter, F. Raes, U. Lohmann, E. Roeckner, and I. Fischer-Bruns (2010), A GCM study of future climate response to aerosol pollution reductions, *Clim. Dyn.*, *34*, 1177–1194, doi:10.1007/s00382-009-0573-0.

Lamarque, J. F., et al. (2010), Historical (1850–2000) gridded anthropogenic and biomass burning emissions of reactive gases and aerosols: Methodology and application, *Atmos. Chem. Phys.*, *10*(15), 7017–7039, doi:10.5194/acp-10-7017-2010.

Lawrence, M. G., P. Jockel, and R. von Kuhlmann (2001), What does the global mean OH concentration tell us?, *Atmos. Chem. Phys.*, *1*(1), 37–49, doi:10.5194/acp-1-37-2001.

Levin, I., et al. (2010), The global SF_6 source inferred from long-term high precision atmospheric measurements and its comparison with emission inventories, *Atmos. Chem. Phys.*, *10*(6), 2655–2662, doi:10.5194/acp-10-2655-2010.

Meinshausen, M., S. C. B. Raper, and T. M. L. Wigley (2011a), Emulating coupled atmosphere-ocean and carbon cycle models with a simpler model, MAGICC6—Part 1: Model description and calibration, *Atmos. Chem. Phys.*, *11*(4), 1417–1456, doi:10.5194/acp-11-1417-2011.

Meinshausen, M., et al. (2011b), The RCP greenhouse gas concentrations and their extensions from 1765 to 2300, *Clim. Change*, *109*(1–2), 213–241, doi:10.1007/s10584-011-0156-z.

Min, S. K., X. B. Zhang, F. W. Zwiers, and G. C. Hegerl (2011), Human contribution to more-intense precipitation extremes, *Nature*, *470*, 378–381, doi:10.1038/nature09763.

Montzka, S. A., M. Krol, E. Dlugokencky, B. Hall, P. Jockel, and J. Lelieveld (2011), Small Interannual Variability of Global Atmospheric Hydroxyl, *Science*, *331*, 67–69, doi:10.1126/science.1197640.

Moss, R. H., et al. (2010), The next generation of scenarios for climate change research and assessment, *Nature*, *463*(7282), 747–756, doi:10.1038/nature08823.

Nakicenovic, N., et al. (2000), *Special Report On Emissions Scenarios: A Special Report of Working Group III of the Intergovernmental Panel on Climate Change*, 599 pp., Cambridge Univ. Press, Cambridge, U. K.

National Research Council (2010), *Greenhouse Gas Emissions: Methods to Support International Climate Agreements*, Natl. Acad. Press, Washington, D. C.

Olivier, J. G. J., and J. J. M. Berdowski (2001), Global emissions sources and sinks, in *The Climate System*, edited by J. Berdowski, R. Guicherit, and B. J. Heij, pp. 33–78, A. A. Balkema, Lisse, Netherlands.

Prather, M. J. (2007), Lifetimes and time scales in atmospheric chemistry, *Philos. Trans. R. Soc. A*, *365*, 1705–1726, doi:10.1098/rsta.2007.2040.

Prather, M., and C. M. Spivakovsky (1990), Tropospheric OH and the lifetimes of hydrochlorofluorocarbons, *J. Geophys. Res.*, *95*(D11), 18,723–18,729, doi:10.1029/JD095iD11p18723.

Prather, M., et al. (2001), Atmospheric chemistry and greenhouse gases, in *Climate Change 2001: The Scientific Basis. Contribution of Working Group I to the Third Assessment Report of the Intergovernmental Panel on Climate Change*, edited by J. T. Houghton et al., pp. 239–287, Cambridge Univ. Press, Cambridge, U. K.

Prather, M. J., et al. (2009), Tracking uncertainties in the causal chain from human activities to climate, *Geophys. Res. Lett.*, *36*, L05707, doi:10.1029/2008GL036474.

Prentice, I. C., et al. (2001), The carbon cycle and atmospheric carbon dioxide, in *Climate Change 2001: The Scientific Basis. Contribution of Working Group I to the Third Assessment Report of the Intergovernmental Panel on Climate Change*, edited by J. T. Houghton et al., pp. 183–237, Cambridge Univ. Press, Cambridge, UK.

Prinn, R., et al. (1992), Global average concentration and trend for hydroxyl radicals deduced from ale gauge trichloroethane (methyl chloroform) data for 1978–1990, *J. Geophys. Res.*, *97*(D2), 2445–2461, doi:10.1029/91JD02755.

Reisinger, A., M. Meinshausen, M. Manning, and G. Bodeker (2010), Uncertainties of global warming metrics: CO_2 and CH_4, *Geophys. Res. Lett.*, *37*, L14707, doi:10.1029/2010GL043803.

Sander, S. P., et al. (2010), Chemical kinetics and photochemical data for use in atmospheric studies, *JPL Publ.*, *10-6*.

Santer, B. D., T. M. L. Wigley, and P. D. Jones (1993), Correlation methods in fingerprint detection studies, *Clim. Dyn.*, *8*(6), 265–276, doi:10.1007/BF00209666.

Spivakovsky, C. M., et al. (2000), Three-dimensional climatological distribution of tropospheric OH: Update and evaluation, *J. Geophys. Res.*, *105*(D7), 8931–8980, doi:10.1029/1999JD901006.

van Aardenne, J. A., F. J. Dentener, J. G. J. Olivier, C. G. M. K. Goldewijk, and J. Lelieveld (2001), A 1° × 1° resolution dataset of historical anthropogenic trace gas emissions for the period 1890–1990, *Global Biogeochem. Cycles*, *15*, 909–928, doi:10.1029/2000GB001265.

van Vuuren, D. P., et al. (2011), The representative concentration pathways: An overview, *Clim. Change*, *109*, 5–31, doi:10.1007/s10584-011-0148-z.

Zwiers, F., and G. Hegerl (2008), Climate change: Attributing cause and effect, *Nature*, *453*, 296–297, doi:10.1038/453296a.

Auxiliary Material Text for 2012GL051440

Reactive greenhouse gas scenarios: Systematic exploration of uncertainties and the role of atmospheric chemistry

Michael J. Prather, Christopher D. Holmes, Juno Hsu

This Auxiliary Material gives a complete list of the factors controlling the past and future budgets and abundances of CH_4, N_2O, and HFC-134a that were used in this analysis. Of the Kyoto-specified GHG, other HFCs can be evaluated similarly to HFC-134a, while SF_6 and the perfluorocarbons are so long lived that their 21st century abundances are not impacted by uncertainties in atmospheric lifetimes. Primary factors are listed in Table A1 and uniquely identified by lower-case letters (a)-(v) and numbers. These factors are independent of one another and we assume they have uncorrelated uncertainties. For each factor, the values and their uncertainties are drawn from published studies, multiple models or lines of evidence, and expert judgment. Errors in each factor are assumed to be normally distributed and uncertainties are given, in absolute and relative (%) values, as one standard deviation (i.e. the 16%-to-84% confidence interval). The first set of primary factors (a-g) describes the atmosphere and relates the observed tropospheric mean abundances to total burden and radiative forcing. Later factors (h-u) identify the reaction rates and lifetimes necessary to derive the anthropogenic budgets and project future abundances. Due to lack of information, the PI to PD change in natural emissions (v) is assigned an equal-sided uncertainty about 1. Data derived primarily from atmospheric measurements, including air from polar ice sheets, are given asterisks (c*, d*, e*, f*, k*). Preindustrial (PI) is taken to be year 1750 per IPCC [*IPCC*, 2007], and present day is year 2010 with current trends based on years 2006-2010.

Derived factors, designated by upper-case letters (A)-(S) in Table A2, are calculated from the primary factors, and thus the probability distributions of their values are assessed by careful combination of the primary values as in the square root of the sums of the squares (RMS) of the independent uncertainties (absolute for additive terms, relative for multiplicative terms, with the method of propagation here denoted by boldface in Table A2) or through Monte Carlo calculation. The first set of derived factors defines the atmospheric burdens (A-D); and the second set, lifetimes and budgets (E-P) culminating in estimates of natural (PI and PD) and anthropogenic (PD) emissions of N_2O and CH_4 (Q-S). Key data from Table A2 are summarized in the main text Table 1.

One often overlooked factor in deriving trace gas budgets is total amount of dry air (a1). We take this value from the ECMWF integrated forecast system as used in our chemistry and transport model [*Prather et al.*, 2011]: average surface pressure including water vapor is 985.5 hPa; for dry air it is 983.0 hPa. Since trace gas abundances are measured as mole fractions relative to dry air, the latter value should be used for air mass. When comparing our N_2O budgets with the Goddard 2-D model [*Hsu and Prather*, 2010; *Fleming et al.*, 2011], discrepancies of 3% occurred because the 2-D model assumed a global mean surface pressure of 1013 hPa. Atmospheric fill factors (c1-c3) for each gas reflect the fall-off in abundance through the stratosphere and are based on observed profiles. With the atmospheric burden in moles (A1) these factors define the burden factors that scale tropospheric mean abundances to total burden (B1-B3).

In calculating the radiative forcing from PI to PD (M1-M2), our uncertainties in CH_4 are similar to AR4, but those in N_2O are twice as large because we included uncertainty in PI abundance. Including only uncertainties in perturbation lifetimes (N1-N2) [*Forster et al.*, 2007;

Prather, 2007] and radiative forcing per ppb (g1-g3), we estimate global warming potential (GWP) (O1-O3) uncertainties of 10% (N_2O) to (13%) (CH_4). GWPs are defined in terms of a static climate with today's chemistry and composition, but they integrate the effect of a pulsed emission over 100 years. Thus, there is considerable additional uncertainty regarding the impact of CH_4 emissions on climate over the next 100 years [*Shine et al.*, 2005; *Reisinger et al.*, 2011] and AR4 estimates GWPs for chemically reactive species to have uncertainties >20% (one sigma) [*Forster et al.*, 2007].

An excel spreadsheet for Tables A1 and A2 is provided. In this spreadsheet, the uncertainties that can be propagated with the simple RMS approach are calculated with formulae, but those requiring MC calculations are given as fixed numbers and colored blue. The Matlab code used in the Monte Carlo calculation is also provided. The MC calculations give similar results to the simple RMS sums used in the spreadsheet, but the MC is required to calculate uncertainties in some derived quantities, particularly the emissions (Q-S), where uncertainties in the propagated quantities are highly correlated. In Table A2, the boldface uncertainty identifies the method of derivation, with both absolute and relative being boldface for MC results.

Auxiliary Material Spreadsheet. Excel spreadsheet (2012GL051440_ Excel.xls) containing data and formulae for propagating derived values and uncertainties in the tables.

Auxiliary Material MATLAB code. The MATLAB programs used for calculating the Monte Carlo results, including projections from the RCP emissions are supplied. The zip file (2012GL051440_matlab.zip) has a main directory with the primary MATLAB script (mc_script.m) that is designed to run 1,000 MC realizations quickly as a test, a second script for 100,000 realizations (this paper, mc_script_100K.m) is also included with the output from it. A directory listing is included in the zipfile and also separately here (2012GL051440_matlab_dir_listing.txt).

Auxiliary Material References

Allan, W., H. Struthers, and D. Lowe (2007), Methane carbon isotope effects caused by atomic chlorine in the marine boundary layer: Global model results compared with Southern Hemisphere measurements, *Journal of Geophysical Research-Atmospheres*, *112*(D4), D04306.

Atkinson, R., D. Baulch, R. Cox, J. Crowley, R. Hampson, R. Hynes, M. Jenkin, M. Rossi, J. Troe, and T. Wallington (2008), Evaluated kinetic and photochemical data for atmospheric chemistry: Volume IV - gas phase reactions of organic halogen species, *Atmospheric Chemistry and Physics*, *8*(15), 4141-4496.

Brook, E. J., L. Mitchell, J. Severinghaus, and S. Harder (2008), Ice core records of the evolution of atmospheric methane in the Holocene, *AGU Fall Meeting 2008* U33B-02

Demore, W. B. (1992), Relative Rate Constants for the Reactions of Oh with Methane and Methyl Chloroform, *Geophysical Research Letters*, *19*(13), 1367-1370.

Dlugokencky, E. J., R. C. Myers, P. M. Lang, K. A. Masarie, A. M. Crotwell, K. W. Thoning, B. D. Hall, J. W. Elkins, and L. P. Steele (2005), Conversion of NOAA atmospheric dry air CH4 mole fractions to a gravimetrically prepared standard scale, *J. Geophys. Res.*, *110*(D13), D18306.

Douglass, A. R., R. S. Stolarski, M. R. Schoeberl, C. H. Jackman, M. L. Gupta, P. A. Newman, J. E. Nielsen, and E. L. Fleming (2008), Relationship of loss, mean age of air and the distribution of CFCs to stratospheric circulation and implications for atmospheric lifetimes, *Journal of Geophysical Research-Atmospheres*, *113*(D14).

Fleming, E. L., C. H. Jackman, R. S. Stolarski, and A. R. Douglass (2011), A model study of the impact of source gas changes on the stratosphere for 1850-2100, *Atmospheric Chemistry and Physics*, *11*(16), 8515-8541.

Forster, P., et al. (2007), Changes in Atmospheric Constituents and in Radiative Forcing, in *Climate Change 2007: The Physical Science Basis. Fourth Assessment Report of the Intergovernmental Panel on Climate Change*, edited by S. Solomon, D. Qin and M. Manning, pp. 129-234, Cambridge University Press, Cambridge UK.

Holmes, C. D., Q. Tang, and M. J. Prather (2011), Uncertainties in climate assessment for the case of aviation NO, *Proceedings of the National Academy of Sciences of the United States of America*, *108*(27), 10997-11002.

Houweling, S., F. Dentener, and J. Lelieveld (2000), Simulation of preindustrial atmospheric methane to constrain the global source strength of natural wetlands, *Journal of Geophysical Research*, *105*(D13), 17243-17255.

Hsu, J., and M. J. Prather (2010), Global long-lived chemical modes excited in a 3-D chemistry transport model: Stratospheric N_2O, NOy, O_3 and CH_4 chemistry, *Geophysical Research Letters*, *37*(7), L07805.

Hsu, K. J., and W. B. Demore (1995), Rate Constants and Temperature Dependences for the Reactions of Hydroxyl Radical with Several Halogenated Methanes, Ethanes, and Propanes by Relative Rate Measurements, *Journal of Physical Chemistry*, *99*(4), 1235-1244.

IPCC (2007), *Climate Change 2007: The Physical Science Basis. Contribution of Working Group I to the Fourth Assessment Report of the Intergovernmental Panel on Climate Change*, 996 pp., Cambridge University Press Cambridge, United Kingdom.

Meure, C. M., D. Etheridge, C. Trudinger, P. Steele, R. Langenfelds, T. van Ommen, A. Smith, and J. Elkins (2006), Law Dome CO2, CH4 and N2O ice core records extended to 2000 years BP, *Geophysical Research Letters*, *33*(14), L14810.

Montzka, S. A., M. Krol, E. Dlugokencky, B. Hall, P. Jockel, and J. Lelieveld (2011), Small Interannual Variability of Global Atmospheric Hydroxyl, *Science*, *331*(6013), 67-69.

NOAA (2011a), Halocarbons & other Atmospheric Trace Species Group (HATS), *http://www.esrl.noaa.gov/gmd/hats/combined/N2O.html*

NOAA (2011b), Annual Greenhouse Gas Index (AGGI), *http://www.esrl.noaa.gov/gmd/aggi/*, aggi_2011.fig2012.png.

Prather, M., and C. M. Spivakovsky (1990), Tropospheric OH and the lifetimes of hydrochlorofluorocarbons, *Journal of Geophysical Research-Atmospheres*, *95*(D11), 18723-18729.

Prather, M., et al. (2001), Atmospheric Chemistry and Greenhouse Gases, in *Climate Change 2001: The Scientific Basis. Third Assessment Report of the Intergovernmental Panel on Climate Change*, edited by J. T. Houghton, Y. Ding and D. J. Griggs, pp. 239-287, Cambridge University Press, Cambridge UK.

Prather, M. J. (2007), Lifetimes and time scales in atmospheric chemistry, *Philosophical Transactions of the Royal Society a-Mathematical Physical and Engineering Sciences*, *365*(1856), 1705-1726.

Prather, M. J., and J. Hsu (2010), Coupling of Nitrous Oxide and Methane by Global Atmospheric Chemistry, *Science*, *330*, 952-954.

Prather, M. J., X. Zhu, Q. Tang, J. N. Hsu, and J. L. Neu (2011), An atmospheric chemist in search of the tropopause, *Journal of Geophysical Research-Atmospheres*, *116*(D4), D04306.

Reisinger, A., M. Meinshausen, and M. Manning (2011), Future changes in global warming potentials under representative concentration pathways, *Environmental Research Letters*, *6*(2), 024020.

Sander, S. P., et al. (2010), Chemical Kinetics and Photochemical Data for Use in Atmospheric Studies, Evaluation Number 17*Rep.*, Jet Propulsion Laboratory, Pasadena, CA.

Shine, K. P., T. K. Berntsen, J. S. Fuglestvedt, and R. Sausen (2005), Scientific issues in the design of metrics for inclusion of oxides of nitrogen in global climate agreements, *Proceedings of the National Academy of Sciences of the United States of America*, *102*(44), 15768-15773.

Spahni, R., et al. (2005), Atmospheric methane and nitrous oxide of the late Pleistocene from Antarctic ice cores, *Science*, *310*(5752), 1317-1321.

Spivakovsky, C. M., et al. (2000), Three-dimensional climatological distribution of tropospheric OH: Update and evaluation, *Journal of Geophysical Research-Atmospheres*, *105*(D7), 8931-8980.

Strahan, S. E., et al. (2011), Using transport diagnostics to understand chemistry climate model ozone simulations, *Journal of Geophysical Research-Atmospheres*, *116*(D17), D17302.

Volk, C. M., J. W. Elkins, D. W. Fahey, G. S. Dutton, J. M. Gilligan, M. Loewenstein, J. R. Podolske, K. R. Chan, and M. R. Gunson (1997), Evaluation of source gas lifetimes from stratospheric observations, *Journal of Geophysical Research-Atmospheres*, *102*(D21), 25543-25564.

Wennberg, P., S. Peacock, J. Randerson, and R. Bleck (2004), Recent changes in the air-sea gas exchange of methyl chloroform, *Geophysical Research Letters*, *31*(16), L16112.

WMO (2010), *Scientific Assessment of Ozone Depletion: 2010*, World Meteorological Organization, Geneva, Switzerland.

Table A1. Primary factors controlling the atmospheric abundance of N_2O, CH_4, CH_2FCF_3

code	primary quantity	gas	value		%	Abs	references and notes
a1	atmospheric mass (Tg)	dry air	**5.113 x10^{9}**	±			based on ECMWF met fields, derived from [*Hsu and Prather*, 2010], <0.5% uncertainty; water vapor mass 1.21x10^{7}
b1	molecular weight (Daltons)	dry air	**28.97**	±			derived from N_2, O_2 and Ar, all molecular weight uncertainties are <0.5%
b2		N2O	**28.0**	±			all N_2O budgets based on Tg-N
b3		CH4	**16.0**	±			
b4		HFC-134a	**102.0**	±			Gas = CH_2FCF_3
b5		MCF	**133.4**	±			Gas = CH_3CCl_3
c1*	fill factor (atmospheric to tropospheric abundance)	N2O	**0.970**	±	1.0%	0.01	LLGHG abundances expressed as tropospheric means; derived from [*Volk et al.*, 1997; *Hsu and Prather*, 2010]
c2*		CH4	**0.973**	±	1.0%	0.01	[*Volk et al.*, 1997; *Hsu and Prather*, 2010]
c3*		HFC-134a	**0.97**	±	2.1%	0.02	Little data on stratospheric HFCs, choose to be like CH_4 but with ±2% uncertainty.
c4*		MCF	**0.92**	±	1.1%	0.01	[*Volk et al.*, 1997]
d1*	Preindustrial (PI) abundance (ppb)	N2O	**270**	±	2.6%	7	from AR4 Fig 6.4 [*IPCC*, 2007]; uncertainty from [*Spahni et al.*, 2005]
d2*		CH4	**700**	±	3.6%	25	based on pre-Industrial Holocene values of 700 ppb (AR4, Chapter 2.3.2, [*Forster et al.*, 2007]); 670-720 ppb [*Meure et al.*, 2006]; 690-725 ppb [*Brook et al.*, 2008]; note value does not include bias correction for different PI vs. PD standard scales [*Dlugokencky et al.*, 2005].
d3*		HFCs	**0**	±	0	0	no natural sources
e1*	Present day (PD = year 2010) abundance (ppb, HFCs in ppt)	N2O	**323**	±	1.0%	3.2	[*NOAA*, 2011a]; ±1% uncertainty to account for integrating tropospheric mean from surface observations.
e2*		CH4	**1795**	±	1.0%	18.0	[*NOAA*, 2011b]; as above.
e3*		HFC-134a	**58**	±	5.0%	2.9	extrapolated from WMO Table 1-15 [*WMO*, 2010] ; ±5% uncertainty (two independent laboratories).
f1*	PD growth rate (ppb/yr)	N2O	**0.8**	±	12.5%	0.1	AR4 Table 2.1[*Forster et al.*, 2007], also [*NOAA*, 2011a]
f2*		CH4	**5**	±	20.0%	1	AR4, Table 2.1[*Forster et al.*, 2007], also [*NOAA*, 2011b]
g1	RF factor (W /m2 /ppb)	N2O	**3.03 x10^{-3}**	±	6.1%	1.8 x10^{-4}	all from AR4 [*Forster et al.*, 2007], changing ±10% (90%-confidence) to ±6.1% (one sigma)
g2		CH4	**3.70 x10^{-4}**	±	6.1%	2.2 x10^{-5}	
g3		HFC-134a	**0.16**	±	6.1%	9.6 x10^{-3}	
h1	temperature (K) for scaling trop-OH reactions		**272**	±	1.8%	5	from [*Spivakovsky et al.*, 2000], uncertainty from change since [*Prather and Spivakovsky*, 1990]
i1	ratio of OH reaction rates at 272K: [OH+gas]/[OH+MCF]	CH4	**0.601**	±	10.0%	0.060	average of 0.585 ±23% [*Sander et al.*, 2010], 0.614 [*Atkinson et al.*, 2008], 0.603 ±7% [*Demore*, 1992; *Hsu and Demore*, 1995]; uses DeMore uncertainty in ratio but increased to ±10%.

i2		HFC-134a	**0.427**	±	10.0%	0.043	HFC reaction rate ratio to MCF [*Sander et al.*, 2010], only uncertainty in the [OH+HFC] rate is used here.
j1	ratio of OH reaction rates at 225K: [OH+gas]/[OH+CH4]	HFC-134a	**0.816**	±	10.0%	0.082	HFC reaction rate ratio to CH4 in stratosphere [*Sander et al.*, 2010], uncertainty as (i2).
k1*	global decay rate (/y)	MCF	**0.181**	±	2.8%	0.005	observed 1998-2007 [*Montzka et al.*, 2011]
l1	stratospheric lifetime (y)	N2O	**131**	±	7.6%	10	[*Douglass et al.*, 2008; *Hsu and Prather*, 2010; *Prather and Hsu*, 2010; *Fleming et al.*, 2011; *Strahan et al.*, 2011] with some new calculations
l2		CH4	**120**	±	20.0%	24	[*Prather et al.*, 2001], uncertainty estimated
l3		MCF	**42.6**	±	14.1%	6	[*Volk et al.*, 1997] scaled to 56-yr CFC-11 lifetime [*Douglass et al.*, 2008], uncertainty estimated
m1	oceanic loss frequency (/y)	MCF	**0.000**	±	n/a	0.0071	with decline in MCF, ocean may be a source [*Wennberg et al.*, 2004]; uncertainty range is lifetime of ±140 y.
n1	lifetime vs. soil uptake (y)	CH4	**150**	±	33.3%	50	[*Prather et al.*, 2001]
o1	lifetime vs. trop-Cl (y)	CH4	**200**	±	50.0%	100	[*Allan et al.*, 2007]
p1	Change in trop-OH, PI:PD	OH	**0.95**	±	10.5%	0.10	from preliminary analysis by V. Naik of the ACCMIP model results UM-CAM, GISS, NCAR, MOCAGE, GFDL, LSCE, GFDL-CM3, UKMO, NCAR-CAM as of 2011 Oct); disagrees with TAR Table 4.11[*Prather et al.*, 2001], which predicts 1.32 from CH$_4$ decrease.
q1	OH lifetime feedback, S = -dln(OH)/dln(CH4)	CH4	**0.32**	±	15.6%	0.05	from TAR Table 4.11 [*Prather et al.*, 2001], with range including [*Holmes et al.*, 2011]; applies only to tropospheric-OH lifetime.
r1	Change in trop-OH, Y2100 : PD, due to NOx, VOC, temperature.	OH	**1.00**	±	15.0%	0.15	estimate of future changes in OH, other than the CH$_4$ feedback (q1).
s1	lifetime(L) feedback, S = dlnL/dlnN2O	N2O	**-0.08**	±	25%	0.02	[*Prather and Hsu*, 2010; *Fleming et al.*, 2011] updated with new calculations. The perturbation lifetime (PT) of a pulse is calculated from this and the lifetime (LT): PT/LT = 1/(1-S).
t1	PI – PD lifetime (y)	N2O	**11**	±	n/a	10	[*Fleming et al.*, 2011], uncertainty to include no change.
u1	Y2100 – PD lifetime (y) due to other than N2O change	N2O	**-2**	±	n/a	6	for SRES A1B [*Fleming et al.*, 2011], large uncertainty from cancelling factors
v1	Change in natural emissions, PI:PD	N2O	**1.00**	±	10%	0.10	See v2
v2		CH4	**1.00**	±	10%	0.10	Uncertainty based on estimated 10% decline in natural wetland sources [*Houweling et al.*, 2000]

Table A2. Derived factors controlling the atmospheric abundance of N_2O, CH_4, CH_2FCF_3

code	derived quantity	gas	value		%*	abs*	derivation and notes
A1	Teramoles per ppb of dry air	dry air	**0.1765**	±		**0**	(a1) / (b1) (*10^{-9}), <0.5% uncertainty
B1	Burden : trop-mean (Tg/ppb)	N2O	**4.79**	±	**1.0%**		(A1) * (b2) * (c1)
B2		CH4	**2.75**	±	**1.0%**		(A1) * (b3) * (c2)
B3		HFC-134a	**17.5**	±	**2.1%**		(A1) * (b4) * (c3)
C1	PD burden (Tg)	N2O	**1548**	±	**1.4%**	22	(B1) * (e1)
C2		CH4	**4932**	±	**1.4%**	71	(B2) * (e2)
C3		HFC-134a	**1.01**	±	**5.4%**	0.05	(B3) * (e3)
D1	PI burden (Tg)	N2O	**1294**	±	**2.8%**	36	(B1) * (d1)
D2		CH4	**1923**	±	**3.7%**	71	(B2) * (d2)
D3		HFC-134a	**0**	±	**2.1%**	0	(B3) * (d3)
E1	ratio of trop-OH loss to MCF	CH4/MCF	**0.601**	±	**10.1%**	0.061	(i1) + 1.7% uncertainty from (h1) propagating through exp(-1775/T) / exp(-1520/T).
E2		HFC-134a	**0.427**	±	**10.0%**	0.043	(i2) + 0.7% uncertainty from (h1) propagating through exp(-1630/T) / exp(-1520/T).
F1	trop-OH inverse lifetime (/y)	MCF	**0.1575**	±	5.9%	**0.0093**	(k1) - 1/(l3) - (m1)
F2		MCF**	**0.1449**	±	**6.0%**	0.0087	(F1) * (c4), normalized to uniform MCF abundance.
F3		CH4**	**0.0871**	±	**11.8%**	0.0103	(F2) * (E1), inverse OH-lifetime for uniform CH_4 abundance.
F4		CH4	**0.0895**	±	**11.8%**	0.0106	(F3) / (c2); OH-lifetime = 11.2 ± 1.3 y
F5		HFC-134a	**0.0638**	±	**11.9%**	0.0076	(F2) * (E2) / (c3).
G1	strat inverse lifetime (/y)	HFC-134a	**0.0068**	±	**22.4%**	0.0015	(j1) / (l2)
H1	total inverse lifetime (/y)	CH4	**0.1095**	±	10.3%	**0.0112**	(F4) + 1/(l2) + 1/(n1) + 1/(o1), lifetime = 9.14 y ± 10%
H2		HFC-134a	**0.0706**	±	10.9%	**0.0077**	(F5) + (G), lifetime = 14.2 y ± 11%
I1	PD loss rate (Tg/y)	N2O	**11.8**	±	**7.8%**	0.9	(C1) / (l1)
I2		CH4	**540**	±	**10.4%**	56	(C2) * (H1)
J1	PD growth rate (Tg/y)	N2O	**3.8**	±	**16.2%**	0.6	(B1) * (f1)
J2		CH4	**14**	±	**25.8%**	4	(B2) * (f2)
K1	PD emissions (Tg/y)	N2O	**15.7**	±	7.1%	**1.1**	(I1) + (J1)
K2		CH4	**554**	±	10.1%	**56**	(I2) + (J2)
L1	PD-PI abundance (ppb, ppt)	N2O	**53**	±	14.5%	**8**	(e1) - (d1)
L2		CH4	**1095**	±	2.8%	**31**	(e2) - (d2)
L3		HFC-134a	**58**	±	5.0%	**3**	(e3) - (d3)
M1	RF: PD-PI (W/m2)	N2O	**0.16**	±	**15.7%**	0.025	Approximated as (L1) * (g1); the RFs for N_2O and CH_4 are non-linear and coupled [*Forster et al.*, 2007]; the key numbers here are the uncertainties.
M2		CH4	**0.40**	±	**6.6%**	0.027	Approximated as (L2) * (g2), see above
M3		HFC-134a	**0.009**	±	**7.8%**	0.001	(L3) * (g3) / 1000
N1	perturbation lifetime (y)	N2O	**121**	±	**7.9%**	9.5	(l1) / [1 - (s1)]
N2		CH4	**12.4**	±	**11.5%**	1.4	1 / [(F4) * [1-(q1)] + 1/(l2) + 1/(n1) + 1/(o1)]
N3		HFC-134a	**14.2**	±	**10.9%**	1.5	1 / (H2)
O1	GWP (100 year)	N2O	**317**	±	**9.9%**	31	298 * (N1) / 114, scaled from AR4, uncertainty in (N1) and (g1)
O2		CH4	**26**	±	**12.9%**	3	25 * (N2) / 12, scaled from AR4, uncertainty in (N2) and (g2).
O3		HFC-134a	**1447**	±	**12.5%**	180	1430 * (N3) / 14, scaled from AR4, uncertainty in (N3) and

							(g3).
P1	PI lifetime (y)	N2O	**142**	±	10.0%	**14**	(l1) + (t1)
P2		CH4	**9.5**	±	**13.3%**	1.3	1 / [(F4) * (p1) + 1/(l2) + 1/(n1) + 1/(o1)]
Q1	PI (natural) emissions (Tg/y)	N2O	**9.1**	±	**10%**	**1.0**	(D1) / (P1), uncertainty from MC calculation.
Q2		CH4	**202**	±	**14%**	**28**	(D2) / (P2), as above
R1	PD (natural) emissions (Tg/y)	N2O	**9.1**	±	**14%**	**1.3**	(Q1) / (v1), uncertainty from MC calculation.
R2		CH4	**202**	±	**17%**	**35**	(Q2) / (v2), as above.
S1	PD anthropogenic emissions (Tg/y)	N2O	**6.5**	±	**26%**	**1.3**	(K1) - (R1), uncertainty from MC calculation.
S2		CH4	**352**	±	**19%**	**45**	(K2) - (R2), as above.

* A boldface uncertainty (% or abs) indicates which uncertainty is derived from the primary uncertainties. If both are bold and blue (Q-R-S) then the MC calculation is used.